Regenerative self-pulsating sources of large bandwidths

Thibault North* and Martin Rochette

Department of Electrical and Computer Engineering, McGill University, Montréal (Québec), H3A 2A7, Canada

**Corresponding author: thibault.north@mail.mcgill.ca*

Received October 14, 2013; revised November 26, 2013; accepted November 28, 2013; posted December 3, 2013 (Doc. ID 199311); published December 24, 2013

Self-pulsating sources based on cascaded regeneration by self-phase modulation and offset filtering are investigated experimentally using large filter bandwidths of 3.5 nm and up to semi-infinite bandwidths. In accordance with numerical results reported previously, such sources self-start from amplified spontaneous emission, and picosecond pulses are sustained in a nonlinear cavity. We provide numerical and experimental results indicating the generation of 2 ps pulses and observe 0.4 ps pulses after dispersion compensation and amplification. We also demonstrate that a pair of low- and high-pass filters spawn pulses whose bandwidths are determined by the combination of the filters and gain profiles, hence simplifying the experimental setup for short pulse generation.

OCIS codes: (060.3510) Lasers, fiber; (140.3510) Lasers, fiber; (190.4370) Nonlinear optics, fibers; (190.5530) Pulse propagation and temporal solitons; (190.5650) Raman effect; (320.5390) Picosecond phenomena.

http://dx.doi.org/10.1364/OL.39.000174

Cascaded reshaping and reamplification regenerators in a closed loop offer an alternative to well-known pulsed fiber lasers based on additive-pulse mode locking [1], semiconductor saturable absorbers [2], or Kerr-lens mode locking [3]. Distinctive features of regenerative sources include aperiodicity, low polarization sensitivity, and built-in spectral broadening, which enables the generation of femtosecond pulses via nonlinear compression [4,5]. Moreover, these sources are able to sustain picosecond pulses in ultralong cavities >2 km and provide multiwavelength pulsed operation in distinct functioning regimes, the self-pulsating (SP) and pulse-buffering (PB) regimes. Regenerative sources are not mode locked: there exists no fixed phase relation between all propagating modes, which enables aperiodicity and therefore is compatible with applications requiring PB. Pulses are initiated from amplified spontaneous emission (ASE) by a saturable absorber effect that relies on consecutive spectral broadening and offset filtering of the circulating signal. The properties of the pulses sustained in the cavity are directly determined by the spectral profiles of the bandpass filters (BPFs), and the nonlinear transfer function of these sources naturally provides high stability [6,7], forming eigenpulses that are close to being chirp-free when the BPFs have a bandwidth <1 nm. In other cases, a linear chirp opposes the decrease in the pulse temporal duration, and propagation in a dispersive medium is required to compress the output pulses down to a chirp-free limit. Previous reports of such sources are limited to an operation with filter bandwidths of 0.9 nm or less. In Ref. [5], the shortest pulses observed without nonlinear compression were at their transform limit, with a duration of 3 ps and an energy of 0.17 pJ. Recently, we reported numerical simulations suggesting that large filter bandwidths were not an obstacle to self-pulsation [8]. On the contrary, less energy is wasted during the regeneration stage because the BPFs transmit a larger amount of spectral components contributing to the pulses in comparison to the use of smaller bandwidth filters.

In this Letter, we report the observation of ultrashort pulses in cavity configurations featuring large filter bandwidths, and hence providing high power efficiency. In this work, near-chirp-free pulses as short as 2 ps and with energies increased by 20× with respect to previous reports are observed without compression or chirp compensation when the filter bandwidth attains 3.5 nm. After propagation in single-mode fiber (SMF) and amplification, the pulses are compressed down to a duration of <0.5 ps. Moreover, we demonstrate that the combination of a low- and high-pass filter composes a functional limiting case of SP sources based on cascaded regeneration, minimizing the amount of discarded spectral components at the expense of the pulse quality. The nonlinear medium used in this work also provides a dispersion profile that favors the ignition of pulses via stimulated Raman scattering (SRS), and hence sustains pulses at the first Stokes wavelength of ∼1670 nm.

The SP cavity under study is depicted in Fig. 1(a) and resembles the design in Ref. [4]. Instead of using BPFs tunable in wavelength only, filters that are adjustable in bandwidth and tunable in wavelength are used. As shown in Fig. 1(b), such filters offer flexibility, but with the downside that their spectral shapes deviate strongly from Gaussian and are best fitted with super-Gaussians. As a consequence of that and by the properties of the Fourier transform, the temporal profile of the output pulses is expected to exhibit a pedestal. The highly nonlinear fiber (HNLF) has a waveguide nonlinear coefficient $\gamma = 11.5\ \mathrm{W^{-1}\,km^{-1}}$, second- and third-order chromatic dispersion coefficients $D = -0.71\ \mathrm{ps/(nm \cdot km)}$ and $S = 0.0074\ \mathrm{ps/(nm^2 \cdot km)}$, respectively, at a wavelength of 1550 nm for a length of $L = 1007$ m. $\mathrm{BPF_1}$ is continuously tunable in bandwidth and wavelength in the C-band and has an insertion loss of 5.5 dB. $\mathrm{BPF_2}$ is adjustable by passing or blocking neighboring channels of 100 GHz. It has an insertion loss of 8 dB. Each circulator has an insertion loss of 2 dB, and each output coupler O_i has an insertion loss of 0.5 dB in addition to the loss resulting from its coupling ratio. The erbium-doped fiber amplifiers (EDFAs) have a saturated output power of ∼15 dBm. Pulses centered at a wavelength of λ_1

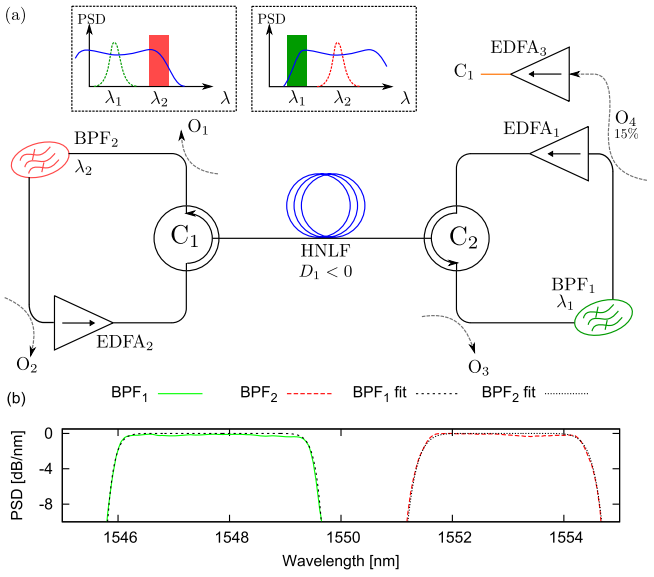

Fig. 1. (a) Experimental setup of the self-pulsating source. Insets: spectral overview of the source operation, including spectral broadening by SPM and offset filtering at wavelengths λ_1 and λ_2. (b) Profiles of the BPFs. BPF, bandpass filter; HNLF, highly nonlinear fiber; EDFA, erbium-doped fiber amplifier; PSD, power spectral density; C_i, circulators; O_i, output tap couplers.

undergo spectral broadening in the HNLF by self-phase modulation (SPM) in a medium featuring normal dispersion. A slice of that spectrum is preserved at BPF_2. Amplification compensates for the loss in power, and the pulses now centered at λ_2 propagate in the HNLF in the opposite direction. Their spectrum is broadened by SPM, and part of that spectrum traverses BPF_1 and is amplified at $EDFA_1$, therefore closing the loop. BPF_1 is shifted toward the long wavelengths to trigger self-pulsation, and then in the opposite direction to attain the PB regime. The source self-starts for any BPF bandwidth smaller than 14.5 nm, which is the upper limit of tunability of BPF_2.

In a first configuration, the bandwidth of BPF_1 is set to 3.5 nm, and the 3 dB edge-to-edge spectral separation between the filters is 1.8 nm. The bandwidth of BPF_2 is 3.2 nm. Output pulses are observed in the time domain via a frequency-resolved optical gating (FROG). These measurements are compared with simulations in Fig. 2. The numerical model includes super-Gaussian filters as described in Fig. 1(b), and the HNLF is modeled including its second- and third-order dispersion coefficients. Nonlinear propagation is modeled with a Runge–Kutta algorithm of order 4 on a GeForce GTX 470 processor, with an adaptive step size [9,10]. The simulation begins from the ASE spectrum sampled from an EDFA in an open-loop configuration. Figure 2 indicates that the pulses generated at a filter bandwidth of 3.5 nm exhibit a near-Gaussian shape with a pedestal. The recovered pulses have a duration of 2 ps, and simulations indicate that dispersion compensation does not enable a significant compression, in contrast with the Gaussian BPFs of Ref. [5]. In case of Gaussian BPFs, the duration of pulses would be 2.6 and 1 ps when the chromatic dispersion is compensated with additional SMF. The

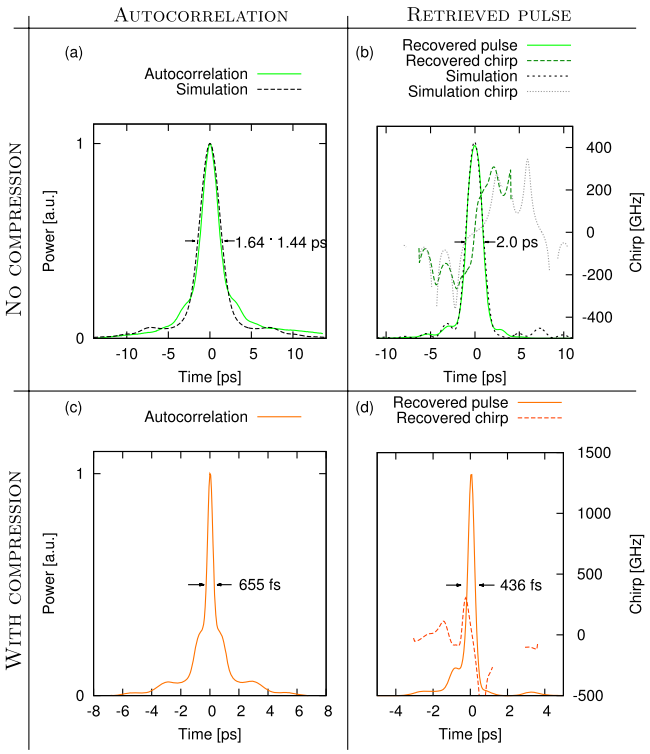

Fig. 2. Pulses observed at O_4 (top row) and C_1 (bottom row) via a FROG. (a) Measured and simulated pulse autocorrelation, (b) FROG-recovered pulse and simulated pulse, (c) autocorrelation of the pulse compressed with additional SMF, and (d) pulses of (c) as retrieved by the FROG.

measured pulse duration corresponds well to the simulation, as depicted in Figs. 2(a) and 2(b). The differences in the chirp values are attributed to the effects of amplification at $EDFA_3$, as well as the residual error in the FROG retrieval algorithm, confirmed by the mismatch between the retrieved pulse duration and the autocorrelation width. Figures 2(c) and 2(d) indicate the autocorrelation width and retrieved pulse profile when the output signal is amplified, and 13 m of additional SMF-28 fiber is appended at O_4. The pulse duration shortens, because nonlinear compression occurs as a consequence of SPM inside $EDFA_3$, followed by the effects of chromatic dispersion of SMF. This measurement differs from the nonlinear compression of Fig. 9

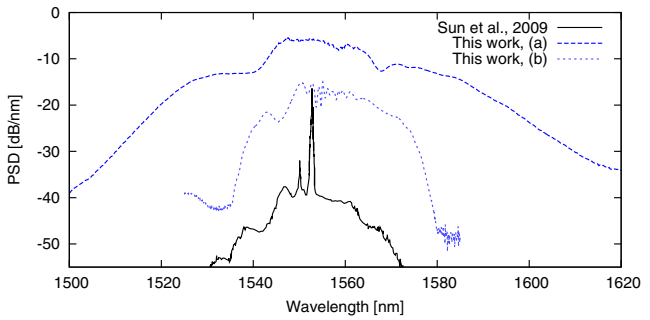

Fig. 3. Comparison of the output spectra originating from this work and previous work by Sun *et al.* [5]. In [5] (solid line), the filter bandwidth was 0.9 nm, and the filter offset was 2.6 nm. In this work, the filter bandwidth is 3.5 nm. In (a) the filter offset is 4.2 nm, and in (b) the filter offset is 5 nm. The reference level of each line was adjusted for visibility.

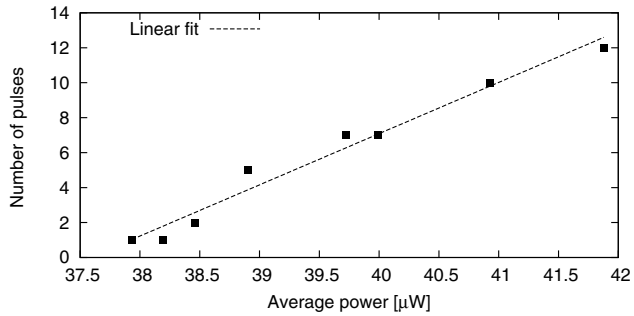

Fig. 4. Number of pulses as a function of the cavity average power observed at O_4.

in Ref. [5], in which pulses were compressed at O_3. In Fig. 3, the output spectra of the source observed at O_1 are shown for two different filter offsets and compared with the pulsed operation of Ref. [5]. The amount of spectral broadening induced by SPM in Fig. 3 in the setup of Sun *et al.* [5] is such that <2% of the power is transferred from λ_2 to λ_1. In (a) and (b), the amount of transferred power is 13% and 15%, respectively. The large 3 dB spectral broadening of 18 nm in (a) and 13 nm in (b) suggests the propagation of powerful and short pulses.

The light propagating in the cavity is composed of ASE and pulses, and the pulse energy is measured when a small number of eigenpulses are visible in the time domain. Since the cavity round-trip time is 10.6 μs, the energy contained in the pulses accounts for only a small portion of the total energy. Under the assumption that the peak power of the pulses does not change significantly when the number of pulses in the cavity changes, the energy is estimated by measuring the average output power as a function of the number of pulses. The decrease in average power is monitored and the number of pulses measured by an oscilloscope through one cavity period. In the current context where the pulse power is small with respect to the total ASE power, the ASE power is expected to remain constant independently of the number of pulses. The energy contained in each pulse can be inferred from the measured average power. In Fig. 4, the filter offset is increased to reduce the pulse number. At output O_4, the energy per pulse is estimated to be 3.5 pJ, considering a pulse duration of 2 ps, and therefore the pulse peak power is 1.7 W at O_4. With a 3 dB spectral separation of 4.5 nm, the cavity contains 12 pulses. This number is small compared with the $>2.9\times10^4$ pulses observed in a similar cavity with filters of 0.9 nm bandwidth and a 3 dB spectral separation of 1.1 nm [5]. However, at a 3.5 nm filter bandwidth, the in-cavity eigenpulse energy is larger than this previous report by a factor of 70.

In a second configuration, the spectral widths of the BPFs are maximized. At these bandwidths, filters BPF_1 and BPF_2 can be considered as high- and low-pass filters, respectively, as their left-most and right-most cut-off edges are outside of the gain window of the EDFAs. In this case, the pulse bandwidth is limited by the gain window on one side and by a filter edge on the other, which permits pulsed operation, as when a pair of BPFs is used. For this configuration, Fig. 5(a) presents the output spectrum of the source in operation. The peak at 1530 nm is

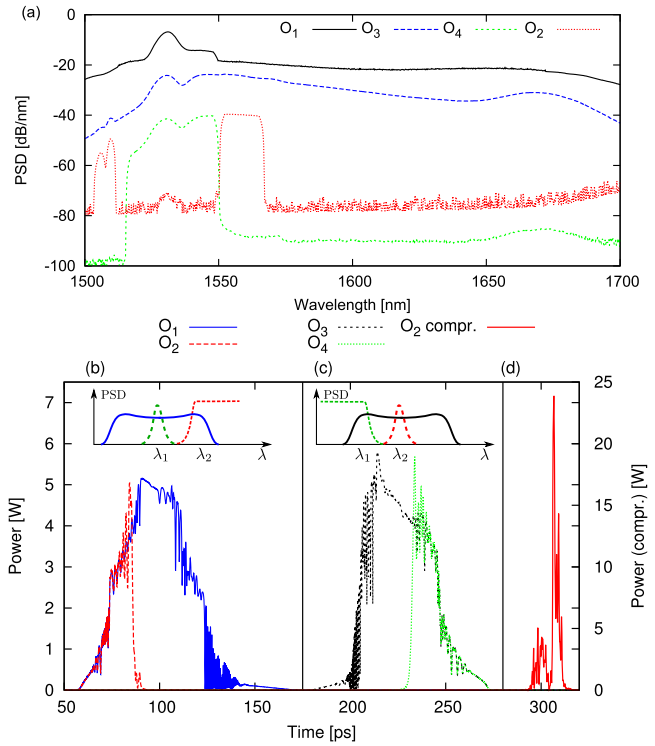

Fig. 5. (a) Experimental spectra before and after bandpass filtering, (b) simulated pulse before and after filtering at BPF_2, (c) simulated pulse before and after filtering at BPF_1, and (d) pulse of (c) compressed by dispersion compensation.

due to the unfiltered EDFA leakage, and BPF_2 fails to block the 1505–1515 nm wavelengths. Figures 5(b) and 5(c) show the simulated pulse profiles in the time domain, before and after filtering at BPF_1 and BPF_2. Because of the propagation in a dispersive HNLF, the spectral components of the pulses spread in time. Only the short wavelengths corresponding to the tail of the pulse are selected after BPF_1, while it is the opposite at BPF_2. Therefore, no single eigenpulse is sustained in the cavity, but rather the alternation of two symmetrical pulses of complex profiles. As depicted in Fig. 5(d), such pulses do not converge toward Gaussians after dispersion compensation. The energy of the filtered pulses of Fig. 5 is of ~50 pJ. Because of SRS, large pulse-to-pulse fluctuations occur, and the autocorrelation trace of such pulses resembles that of noise inside a Gaussian envelope. A positive third-order dispersion coefficient leads to an asymmetry in the spectra broadened by SPM, tilting its top clockwise with respect to the central wavelength [11]. The HNLF generates a Raman replica of the pump pulses at the Stokes wavelengths when the pulse peak power is above the Raman threshold. This is due to a group-velocity matching provided at wavelengths of 1550 nm for the pump and 1670 nm for the Raman signal. Because of the alternative filtering, the Stokes pulses are not sustained in the cavity, but rather rebuilt from noise at each passage through the nonlinear medium. The overlap between the spatial distribution of the pump and Stokes pulses is verified with a broadband InGaAs photodiode and a cascade of two 1310/1550 wavelength-division multiplexers. The pump and Stokes wavelengths are alternately filtered out: the filtering

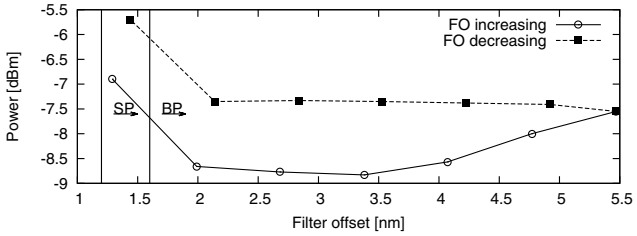

Fig. 6. Domains of self-pulsation (SP) and pulse-buffering (PB) as a function of the filter offset, at output O_4. FO, 3 dB filter offset.

provides an attenuation in excess of 18 dB for each signal. Nevertheless, the pulses propagating in the cavity are visible in both cases, and their respective temporal distribution is similar. This effective transfer of energy toward the Stokes wavelengths induced by the long interaction distance turns into a drawback for the laser cavity efficiency. The energy of the pump pulses transfers toward the Raman pulses, thus leaving less power in the cavity. The polarization dependence of the Raman gain also introduces polarization-dependent losses in the cavity, which is sensitive to external disturbances. In Fig. 6, the tunability of the source is investigated with the largest bandwidths enabled by the adjustable filters. As the filter offset increases, the number of pulses in the cavity first increases as the source efficiency increases. The PB regime is sustained up to a filter offset of 5.5 nm, instead of the ~18 nm predicted by simulations of [8], in the case of Gaussian filters. The energy lost at the pump by SRS and the sharp edges of the BPFs are responsible for this difference.

In conclusion, we have demonstrated that SP sources based on cascaded regeneration operate efficiently using BPFs with transmission windows broader than 1 nm, as previously suggested by numerical simulations. By design, this source toggles in between two wavelengths, 1548 and 1553 nm, as well as generating pulses at 1670 nm via SRS in the HNLF. When BPF_1 and BPF_2 are high- and a low-pass filters, respectively, the gain window determines the spectral bandwidth of the pulses. A simplified cavity could be designed with such components, at the expense of the pulse quality. Despite the nonoptimal filter shapes, pulses of 2 ps as well as pulses shorter than 0.5 ps are observed at the output of the cavity. Regenerative sources therefore operate at large filter bandwidths and are robust to nonoptimal filter shapes.

The authors are thankful to Pierre Galarneau for fruitful discussions and the National Optics Institute (INO) in Quebec City for their financial support.

References

1. E. P. Ippen, H. A. Haus, and L. Y. Liu, J. Opt. Soc. Am. B **6**, 1736 (1989).
2. Y. Silberberg, P. W. Smith, D. J. Eilenberger, D. A. B. Miller, A. C. Gossard, and W. Wiegmann, Opt. Lett. **9**, 507 (1984).
3. D. E. Spence, P. N. Kean, and W. Sibbett, Opt. Lett. **16**, 42 (1991).
4. M. Rochette, L. R. Chen, K. Sun, and J. Hernandez-Cordero, IEEE Photon. Technol. Lett. **20**, 1497 (2008).
5. K. Sun, M. Rochette, and L. R. Chen, Opt. Express **17**, 10419 (2009).
6. P. Mamyshev, in *24th European Conference on Optical Communication* (IEEE, 1998), Vol. **1**, pp. 475–476.
7. S. Pitois, C. Finot, L. Provost, and D. Richardson, J. Opt. Soc. Am. B **25**, 1537 (2008).
8. T. North and M. Rochette, J. Lightwave Technol. **31**, 3700 (2013).
9. J. Hult, J. Lightwave Technol. **25**, 3770 (2007).
10. A. Heidt, J. Lightwave Technol. **27**, 3984 (2009).
11. S. Ghafoor and P. Petropoulos, in *2010 2nd International Conference on Computer Technology and Development (ICCTD)*, Cairo, Egypt , 2010, pp. 144–148.